A Molecular Modeling Study of the Catalytic Mechanism of Haloalkane Dehalogenase: 1. Quantum Chemical Study of the First Reaction Step

Jiří Damborský,*[,†,‡] Michal Kutý,[†,§] Miroslav Němec,[‡] and Jaroslav Koča[†,§]

Laboratory of Biomolecular Structure and Dynamics and Department of Organic Chemistry, Faculty of Science, Masaryk University, Kotlářská 2, 611 37 Brno, Czech Republic, and Department of Microbiology, Faculty of Science, Masaryk University, Tvrdého 14, 602 00 Brno, Czech Republic

Received September 23, 1996[⊗]

The haloalkane dehalogenase of soil bacteria *Xanthobacter autotrophicus* is an enzyme, which catalyzes the environmentally important detoxification process, namely—the hydrolytic cleavage of the carbon−halogen bond. A molecular modeling study has been conducted with the structures of the wild-type enzyme and its mutants in order to investigate the mechanisms of the dehalogenation reaction at molecular level. Semiempirical quantum chemical calculations have been applied to elucidate the importance of the active site residues for kinetic and thermodynamic characteristics in the first step of dehalogenation reaction. The results obtained from these calculations have been compared with previously published experimental results. The strength of the application of molecular modeling method for the study of the evolutionary aspects of biodegradation of organic pollutants is discussed.

INTRODUCTION

Recent advances in DNA-recombinant technology, X-ray crystallography, and NMR spectroscopy make it possible to understand enzymatic reactions at molecular level. Various methods of site-directed mutagenesis are often used to determine the importance of the amino-acid residues inside the enzyme active site for biologically catalyzed reactions—namely for their specificity and activity. Both of these characteristics of the enzymatic reactions are of crucial interest in the case of environmentally important detoxification processes, where the observed recalcitrance of some xenobiotic compounds may be due to, among other things, a missing catalyst.[1,2] The determination of the rate-limiting step of a particular biodegradation reaction is of interest also for Quantitative Structure−Biodegradability Relationships analyses.[3,4]

Molecular modeling methods can be applied in parallel to laboratory experiments and provide useful information about the studied biochemical process. Presently, molecular modeling is used to address biochemical problems in medicinal chemistry.[5] Less common is its application for tackling problems in environmental sciences although there is an obvious analogy in terms of the objects of interest—small organic molecules interacting with the biopolymers. We believe there is an objective need to validate some of the molecular modeling techniques predominantly used at present in drug design to study the mechanisms of processes of environmental concern, like the microbial degradation of organic compounds at a molecular level.[6] Binding of the drug to the enzyme or receptor is the usual process investigated during drug development,[7] while both binding and chemical conversion are important for biodegradation of xenobiotic compounds. Therefore, the tools of computational chemistry, suitable for the study of covalent bond breaking and formation,[8] need to be applied in addition to those for the study of nonbonding interactions.

Haloalkane dehalogenase, the enzyme which is isolated from soil bacteria *Xanthobacter autotrophicus* GJ10,[9] catalyzes the hydrolytic cleavage of the carbon−halogen bond of various haloaliphatic compounds resulting in the replacement of the halogen substituent by a hydroxyl group. This enzyme has been recently intensively studied in terms of its substrate specificity,[10] genetics,[11,12] structure,[13,14] and catalytic mechanism.[15−19] The dehalogenation catalyzed by the haloalkane dehalogenase proceeds in a two-step reaction involving ester intermediate formation (Figure 1) and its subsequent cleavage by a water molecule. Although, the latter step has been suggested to be rate limiting in a wild-type enzyme, based on deuterium oxide kinetic effect measurements, it has been shown that the first reaction step can limit the overall reaction rate in the mutant enzymes with replaced Trp125 and Trp175 residues.[20] The three-dimensional structure of dehalogenase showed that in the active-site the aromatic ring nitrogen atoms of Trp125 and Trp175 point toward the cavity. Further crystallographic and fluorescence measurements[16] showed that the halide ion is bound between the two tryptophans. It was suggested therefore that both residues could be involved in the dehalogenation reaction.

The application of quantum chemical calculations for the modeling of the first reaction step of the dehalogenation reaction is described in this article. The role of tryptophans 125 and 175 for the reaction kinetics and thermodynamics has been elucidated using comparisons of the reaction pathways calculated for the wild-type enzyme with pathways of the model enzymes of single-point mutants.

METHODS

Software and Hardware. The basic manipulation and preparation of the structures for calculation was done using the molecular modeling package InsightII (BIOSYM Technologies, Inc., San Diego CA, 1995), running on workstation SGI Indigo Extreme. Minimization was performed with Discover CVFF force field (BIOSYM Technologies, Inc., San Diego CA, 1995). The semiempirical quantum chemical

† Laboratory of Biomolecular Structure and Dynamics.
§ Department of Microbiology.
‡ Department of Organic Chemistry.
⊗ Abstract published in *Advance ACS Abstracts,* April 1, 1997.

S0095-2338(96)00483-0 CCC: $14.00

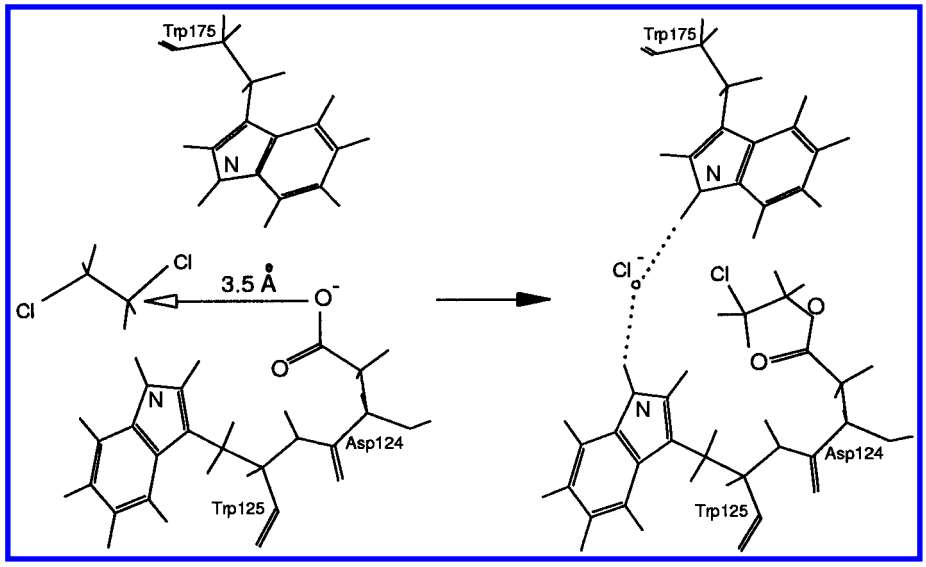

Figure 1. First step of the dehalogenation reaction of haloalkane dehalogenase—formation of the ester intermediate. The deprotonated oxygen atom of aspartic acid 124 undergoes a nucleophilic attack on the substrate (1,2-dichloroethane) carbon atom resulting in the formation of ester intermediate and the release of a chlorine anion, which is most probably stabilized between two partially positively charged N-bound hydrogen atoms of the tryptophans 125 and 175. The mechanism was proposed by Verschueren et al.[15] and further investigated by Priest et al.[17] The coordinate varied (driven) in the calculation is indicated by open arrow. The distance between the reacting atoms was 3.5 Å.

Table 1. Input Structures Used in the MOPAC/DRIVER Calculations

input structure	residues[c] + ligand	enzyme
nucleophile[a]	Asp124 + DCE[d]	wild-type
tryptophans[a]	Asp124, Trp125, Trp175 + DCE	wild-type
tryptophans-m1[b]	Asp124, Phe125, Trp175 + DCE	Trp125→Phe
tryptophans-m2[c]	Asp124, Gln125, Trp175 + DCE	Trp125→Gln
tryptophans-m3[b]	Asp124, Arg125, Trp175 + DCE	Trp125→Arg
tryptophans-m4[b]	Asp124, Trp125, Gln175 + DCE	Trp175→Gln
tryptophans-m5[b]	Asp124, Trp125, Phe175 + DCE	Trp175→Phe
cavity[a]	Glu56, Asp124, Trp125, Phe128, Phe164, Phe172, Trp175, Phe222, Pro223, Val226, Asp260, Leu262 His289 + DCE	wild-type

[a] The coordinates for all residues have been taken from the PDB 2dhc file (wild-type enzyme; see Figure 2). [b] The coordinates of Asp, DCE, and one of the tryptophans have been taken from the PDB file, while the coordinates of the second tryptophan have been obtained by modeling (single point mutants). [c] Numbering according to the haloalkane dehalogenase sequence. [d] DCE = 1,2-dichloroethane.

package MOPAC version 6.0[21] was used to calculate the S_N2 reaction pathway using the new DRIVER technology.[22] The MOPAC/DRIVER calculations were performed on an SGI Power-Challenge XL computer. The output structures were animated with XMol software, version 1.3.1, Minnesota Supercomputer Center, Minneapolis MN, 1993.

Preparation of the Starting Geometries. The Cartesian coordinates of the enzyme−substrate complex of *Xanthobacter autotrophicus* GJ10 haloalkane halidohydrolase soaked with 1,2-dichloroethane (DCE) at pH 5 and 4 °C (educt bound in the active site) were obtained from the Brookhaven Protein Database (PDB accession name 2dhc). Input structures of various complexities were used in the MOPAC/DRIVER calculations (Table 1, Figure 2). A compromise between the size of the system which could be treated by quantum chemical methods, and the reproducibility of obtained results was made. For this purpose all the residues (i) in direct contact with DCE, (ii) surrounding the active site cavity, and (iii) some others suggested to be important for the mechanism of the dehalogenation reaction[14] were included in the "*cavity*" structure.

The structures of the mutants were prepared by substitution of the single amino acid (either of the tryptophan residues) in the structure of the protein−ligand complex. The first four mutants (structures: "*tryptophans-m1, tryptophans-m2, tryptophans-m3, and tryptophans-m4*") are the same as those described in the paper of Kennes.[20] The mutant "*tryptophans-m5*" has been added to represent the structure of the haloalkane dehalogenase isolated from the strain *Sphingomonas paucimobilis* UT26. The sequence of the enzyme of the UT26 strain is known,[23] and the hypothetical three-dimensional structure is proposed by homology modeling.[24] The position of each of the substituted residues within the enzyme structure was adjusted by 1000 minimization steps of the steepest-descent algorithm in Discover. The remainder of the protein molecule was constrained during the minimization to prevent distortion of the X-ray structure. The position of the side chains of the amino acids in close contact with "mutated" residues was not treated by the minimization procedure since most of them were not included in the structures entering the MOPAC calculation and those which were included in the *cavity* or "*tryptophans*" structures adopted their optimal position during the very first step of the MOPAC/DRIVER calculation. C and N terminals of the residues were adjusted by hydrogen atoms to saturate the valences prior to the minimization. Histidine residues were doubly protonated. The protonation state suggested by Verschueren et al.[15] has been used for His289. This residue needs to be singly protonated in order to assume its role during the later stages of dehalogenation reaction (hydrolysis of alkyl-enzyme intermediate).

Calculation of a Reaction Pathway: MOPAC/DRIVER Methodology. The subroutine DRIVER[22] of the semiempirical quantum chemical program MOPAC[21] was used for the mapping of the reaction pathway of the first step, alkyl-enzyme formation, of the dehalogenation reaction catalyzed by the haloalkane dehalogenase (Figure 1). In this subroutine, the internal reaction coordinate is continuously moved from educts to products by a positive step. After each step, the structure is fully optimized with the exception of the driven coordinate. The distance between the nucleophilic

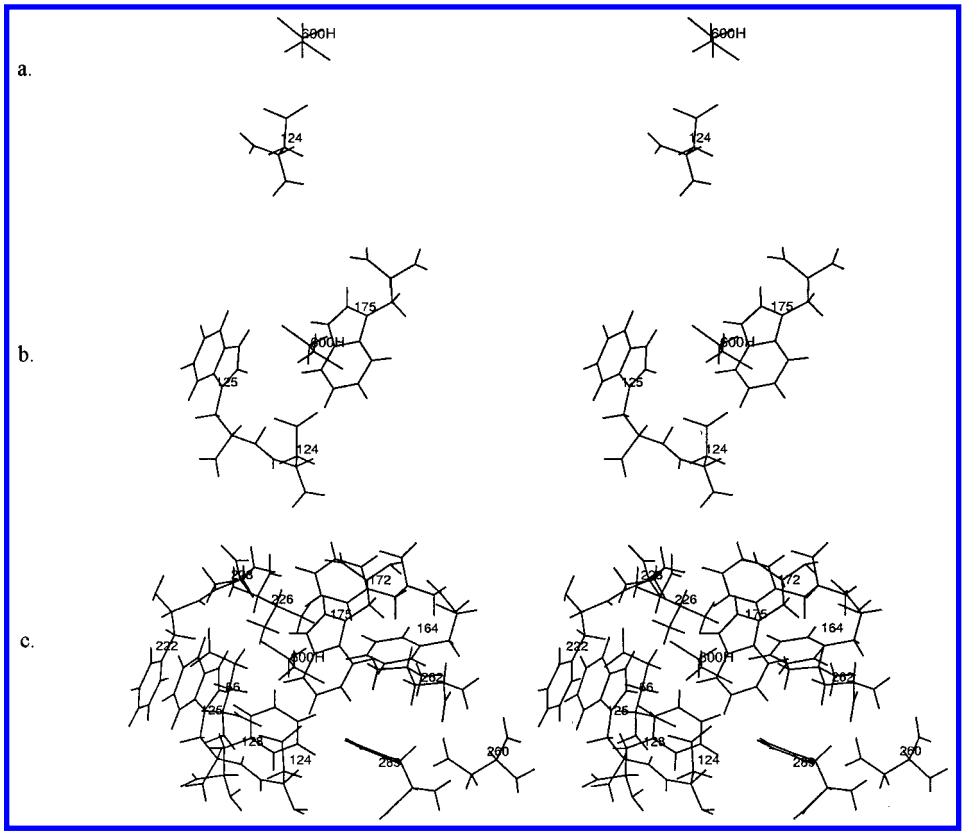

Figure 2. Stereoview of the input structures of the wild-type enzyme used in the calculations: a. *nucleophile*, b. *tryptophans*, and c. *cavity*. The amino acid residues and DCE molecule (600H) are numbered according to 2dhc file obtained from the Brookhaven Protein Database and corresponds to the numbering used in Table 1.

oxygen of aspartic acid (Asp124) and the carbon atom of 1,2-dichloroethane (DCE) was allowed to decrease by defined increments. Increments of the size 0.05 Å were used in calculations with *"nucleophile"* and *tryptophans* structures, while increments of 0.1 and 0.06 Å, respectively, were used in the calculations with *cavity* structure. The following keywords were used to control the MOPAC calculation: AM1; DEBUG; DRIVER; GEO-OK; CHARGE; MMOK; NODIIS; NOINTER; NOXYZ; PRECISE. A very good performance of the MOPAC/DRIVER methodology for localization of the structures close to the transition states has been previously observed for calculations applying small increments.[22] The AM1 Hamiltonian was used throughout the all calculations. The AM1 method appears to be reasonably well parametrized for S_N2 reaction mechanism employing halogen atoms and was shown to correctly reproduce experimental activation energetics of the S_N2 reaction of Cl^- and CH_3C.[25] In addition, the AM1 method reproduces in a reasonably satisfactory manner hydrogen bonds which is of utmost importance for any calculation involving protein systems.[26] The AM1 method has been sucessfully used for modeling the enzyme reaction mechanism of carboxypeptidase A and was found to give excellent energetic results.[27] The parallel calculations with AM1, PM3, and *ab initio* (DFT/6-31G**) methods were performed on simple model structures (1,2-dichloroethane and aspartic acid) to further test the suitability of the method for type of molecules involved in the calculation of the reaction pathways. The resulting geometries and energetics are summarized in Table 2.

Two kinds of constraints were used: (i) fixed backbone of all amino acid residues and (ii) all atoms were constrained (both side chains and backbone) for all the residues except the nucleophile (only the backbone was fixed for the nucleophile). Constrained atoms are included in the MOPAC calculation but do not undergo a change in position during the minimization procedure. No significant difference in terms of activation energy (E^a) and enthalpy difference (ΔH) values was found for the two types of fixation in the case of the *tryptophans* structure (both wild-type and mutants) reported in Table 3. The treatments differed only in the overall shape of the reaction pathways.

Table 2. Comparison of the Ionization Potential and Geometries Obtained with Different Methods Employed on Simple Model Systems[a]

			AM1	PM3	DFT/6-31G**
E[b]	IP	eV	5.26	5.29	0.16
	bond length $C_{ASP}-O_1$	Å (10^{-10} m)	1.26	1.25	1.23
	bond length $C_{DCE}-Cl$	Å (10^{-10} m)	1.51	1.49	1.51
	angle $O_1-C_{ASP}-O_2$	° (deg)	122.32	121.57	128.88
	angle $C_{DCE}-C_{DCE}-Cl$	° (deg)	112.81	109.35	103.94
P[b]	IP	eV	10.44	9.81	4.94
	bond length $C_{ASP}-O_1$	Å (10^{-10} m)	1.23	1.21	1.23
	bond length $C_{ASP}-O_2$	Å (10^{-10} m)	1.37	1.37	1.34
	angle $O_1-C_{ASP}-O_2$	° (deg)	119.45	120.29	122.03
	angle $C_{ASP}-O_2-C_{DCE}$	° (deg)	118.03	119.72	115.28

[a] Model systems were 1,2-dichloroethane (DCE) and aspartic acid (Asp124); input geometries for the ground state were taken were taken from the 2dhc PDB file; product geometry was taken from the calculation of reaction pathway in the *cavity* system and minimized by either method. [b] E, educts; P, products.

Program XMol was used to display and animate the result from the MOPAC/DRIVER calculation. The animation of the chemical reaction step by step provides qualitative information regarding the flexibility of both the ligand molecule and the side chains of the protein active site residues.

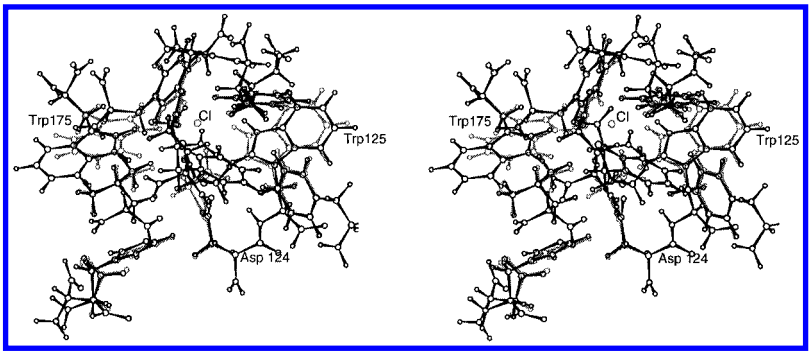

Figure 3. Stereoview of the superimposed structures of two subsequent steps obtained from the MOPAC/DRIVER calculation. The superimposed *cavity* structures of steps 17 and 18 demonstrate the second stage of Trp125 and Trp175 displacement. The geometries were obtained from the MOPAC/DRIVER calculation using 0.1 Å increments. Step 17 (in black) represents the geometry closest to the transition state of the reaction when the carbon atom of DCE is approaching the oxygen atom of Asp124 and is characterized by the C−O distance 1.88 Å, while step 18 (in grey) is characterized by the release of the chlorine ion from DCE and the C−O distance 1.78 Å. The root mean squared deviation (rmsd) between the structures of step 17 and 18 calculated for the tryptophans 125 and 175 was 1.396 compared to 0.191 calculated for the rest of the *cavity* residues (Glu56, Asp124, Phe128, Phe164, Phe172, Phe222, Pro223, Val226, Asp260, Leu262, and His289).

RESULTS AND DISCUSSION

Displacement of the Tryptophan Side Chains During the Reaction Calculation. A significant displacement of the side chains of two tryptophan residues (Trp125 and Trp175) during the reaction calculation with a *cavity* structure and nonfixed side chains was noticed. The same result was obtained several times in different runs of the MOPAC/DRIVER calculation. The position of tryptophan side chains was monitored along the reaction pathway and revealed two stages of displacement. The first one was noticed during the very first step of the minimization procedure, suggesting that the orientation of the tryptophan side chains in the native protein structure is not energetically favorable. Such orientation of tryptophan side chains in protein structure is made possible due to additional stabilization by the surrounding residues which were not considered in the calculation. For example, the aromatic rings of Trp175 are in orthogonal orientation with respect to the aromatic rings of Trp194. This T-tilted arrangement is favored because of the favorable interaction of the partially positively charged H atoms on the edge of one ring with the π-electrons and partially negatively charged C atoms of the face of the other.[28]

The second stage of the displacement (see Figure 3) was noticed in the structure close to the transition state. Changes in position of the tryptophan side chains were correlated with the changes in the position of the halide ion released from the DCE molecule. The tryptophan side chains adopted more or less the same positions as in the original starting structure and which correspond to their orientation in the native protein. This observation suggests that the geometry of the protein active-site is "designed" to bind the transition state rather than ground state of substrate molecule. Trp125 and Trp175 apparently adopt an orientation in the native protein structure that their slightly positively charged nitrogen-bound hydrogens are pointing toward the enzyme active-site in order to secure optimal stabilization of the transition state and the leaving—negatively charged—halide ion. The tryptophan side chains are fixed in their orientation by the surrounding residues. Once these residues are removed and the structure minimized as in case of our calculation, the tryptophans 125 and 175 change their orientation to adopt geometry which is more optimal for the ground state structure. This interpretation corresponds with our more recent results from molecular dynamic simulations of haloalkane dehalogenase in water solution (Linssen, T.; Damborský, J.; Berendsen, H. J. C. Unpublished results).

Since the interaction between the nitrogen-bound hydrogen atoms of the tryptophans and the halide ion was anticipated to be electrostatic in nature, changes in the charges on HNE1 atoms of Trp127 and Trp175 residues during the reaction course were monitored. For this purpose the partial atomic charges from the MOPAC/DRIVER calculation with the *cavity* structure have been extracted. Some of the atomic charges for all 23 reaction steps are plotted on Figure 4. A significant change in atomic charges, mainly between the steps 17 and 18, can be seen for those hydrogen atoms which are expected to exhibit an electrostatic interaction with Cl^- (pointing toward ion), while no change has been observed for the hydrogen atoms on the opposite site of aromatic ring which was used as a control. In addition to the nitrogen-bound hydrogen atoms (HNE1) of Trp125 and Trp175 also one of the hydrogen atoms on the aromatic ring of Phe172 (HE1) also exhibited a significant change in charge during the halide ion release. This Phe172 residue is most probably an additional residue which is important for transition state and/or halide ion stabilization.

Tryptophan Residues 125 and 175 Considerably Improve the Kinetics of the First Step of the S_N2 Dehalogenation Reaction. Independently on the interpretation of the reasons leading toward the tryptophans displacements in the calculation, observed displacement clearly suggest the importance of both tryptophan residues for the reaction mechanism and let us further investigate their contribution toward the transition state and the final intermediate stabilization. Reaction pathways of the first step of the dehalogenation reaction (intermediate ester formation) obtained in the MOPAC/DRIVER calculation with *nucleophile*, *tryptophans*, and *cavity* structures have been compared. The aligned reaction pathways are shown on Figure 5, where the distance of the oxygen atom of nucleophile from the attacked carbon atom of DCE (horizontal axis) is plotted against the relative energy indicating the changes in heat of formation during the reaction (vertical axis).

An endothermic reaction was observed when only the nucleophile and substrate (DCE) were included in the calculation (structure *nucleophile*). Significant changes in kinetic characteristics were observed when both tryptophans together with the nucleophile and DCE were considered in the calculation (structure *tryptophans*). The activation energy

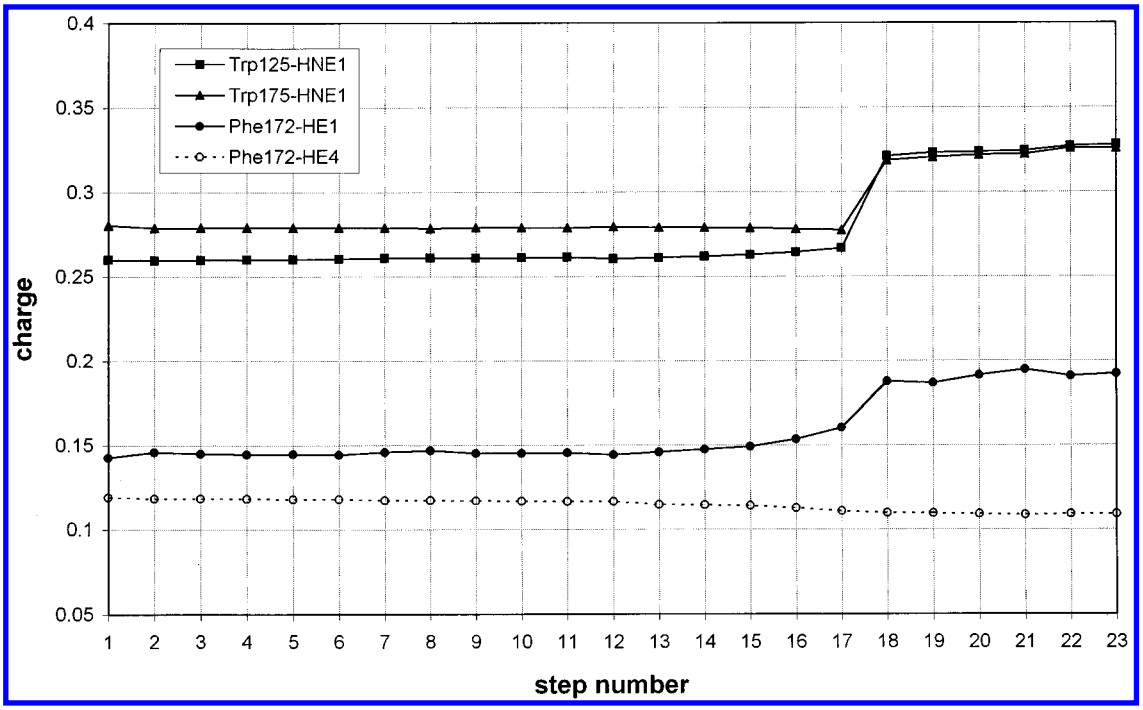

Figure 4. Changes in total atomic charges during the dehalogenation reaction. Charges has been calculated by the AM1 semiempirical method. Step numbers plotted on the horizontal axis refer to the steps in MOPAC/DRIVER simulation with the *cavity* structure using 0.1 Å gradient. Step 17 corresponds to the calculated geometry of the transition state. Trp125-HNE1, Trp175-HNE1, and Phe172-HE1 hydrogen atoms display a large change in the charge value between the steps 17 and 18 corresponding to the electrostatic interaction with the released ion stabilization while the Phe172-HE4 hydrogen atom is used for comparison (no electrostatic interaction expected).

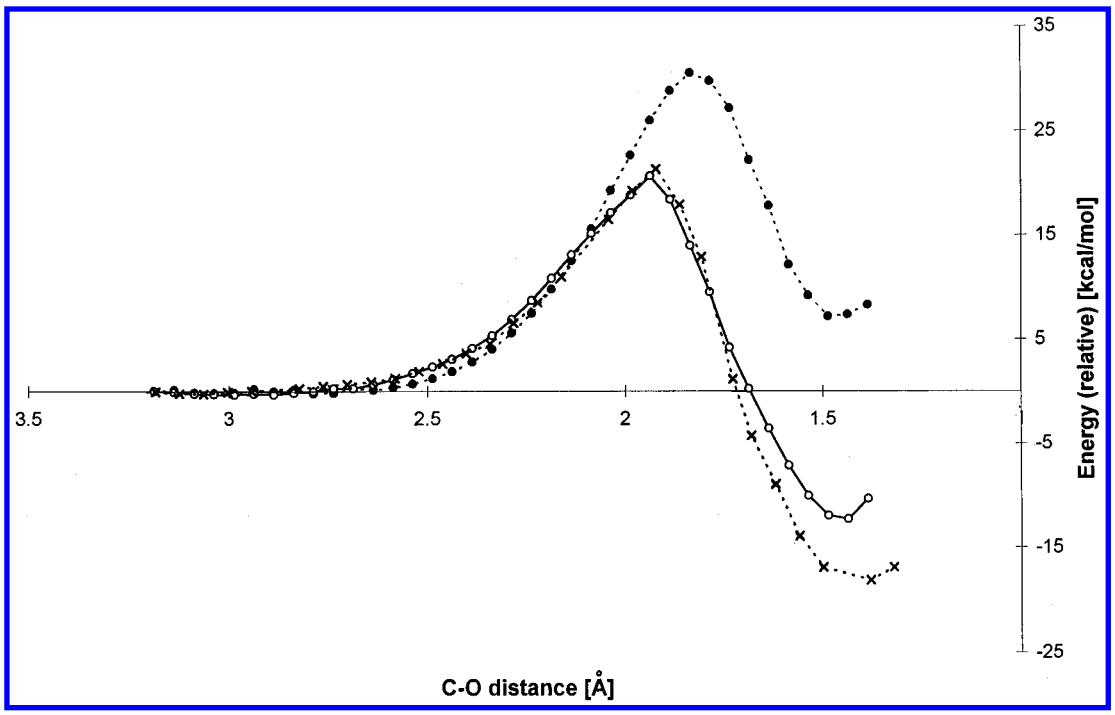

Figure 5. Reaction pathways from the MOPAC/DRIVER calculation obtained with different complexities of the input structures. *Nucleophile* structure (Asp124 + DCE), closed circles and broken line; *tryptophans* structure (Asp124, Trp125, Trp175 + DCE) open circles and full line; *cavity* structure (Glu56, Asp124, Trp125, Phe128, Phe164, Phe172, Trp175, Phe222, Pro223, Val226, Asp260, Leu262, His289 + DCE), crosses and broken line. The C−O distance refers to the distance of the Asp124 nucleophilic oxygen from the DCE electrophilic carbon atom. The energy (heat of formation) of the minimized geometry in each step has been calculated by the AM1 semiemperical method.

of the reaction dropped from 31 to 21 kcal/mol improving substantially the kinetic performance of the reaction.

The calculation of the reaction with the structure *cavity* incorporates some other residues, which form the cavity of the enzyme active site, in the input geometry. No significant changes in the activation energy were observed when comparing the results obtained with *tryptophans* and *cavity* structures, whilst a more favorable ΔH (−17 kcal/mol) was obtained for the *cavity* structure, indicating that the reminder of the active-site residues contribute to the stabilization of the intermediate rather than the transition state.

Comparison of Kinetic and Thermodynamic Parameters Calculated for the Wild-Type and Mutant Structures. Four different mutants of the haloalkane dehalogenase

Table 3. Dehalogenation of the Substrates 1,2-Dichloroethane and 1,2-Dibromoethane by Wild-Type Haloalkane Dehalogenase and Tryptophan Mutants: Experiment versus Quantum Chemical Calculation

			calculation[b]	
input structure	enzyme	experiment[a] V_{max} mmol/min/mg	E^a, kcal/mol	ΔH, kcal/mol
		1,2-Dichloroethane		
tryptophans	wild-type	5.30	21.00	−12.00
tryptophans-m1	Trp125 → Gln	0.15	26.00	−4.00
tryptophans-m2	Trp125 → Phe	1.80	27.00	−5.00
tryptophans-m3	Trp125 → Arg	*c*	*d*	*d*
tryptophans-m4	Trp175 → Gln		31.00	−4.00
tryptophans-m5	Trp175 → Phe	*e*	28.00	−4.00
		1,2-Dibromoethane		
tryptophans	wild-type	4.80	24.00	−8.00
tryptophans-m1	Trp125 → Gln	0.31	28.00	−1.00
tryptophans-m2	Trp125 → Phe	4.40	31.00	2.00
tryptophans-m3	Trp125 → Arg	*c*	*d*	*d*
tryptophans-m4	Trp175 → Gln	0.54	35.00	3.00
tryptophans-m5	Trp175 → Phe	*e*	34.00	0.00

[a] Michaelis−Menten kinetic constant as determined experimentally by Kennes and co-workers.[20] [b] Energy barriers from the MOPAC/DRIVER AM1 calculations. [c] No activity detectable at 10 mM substrate. [d] Reaction did not proceed under conditions described in the METHODS section. [e] Not determined.

have been experimentally prepared by Kennes and co-workers[20] in order to investigate the importance of the tryptophan residues for the dehalogenation reaction. They used two substrates: 1,2-dichloroethane and 1,2-dibromoethane (DBE) in the dehalogenation experiments which lead to the determination of the Michaelis−Menten kinetic constants. We have modelled the structures of the corresponding mutants (plus an additional one, see Methods section) and performed the MOPAC/DRIVER calculations on them. Both the experimental and modeling results are summarized in Table 3. The relationship between activation energy (E^a) and the rate constant (k, experimentally estimated by V_{max}) is given by Arrhenius Law

$$k = Ae(-E^a/RT)$$

where A is the pre-exponential Arrhenius term, R is gas constant, and T is temperature. Activation energies were approximated with quantum-chemically calculated heats of formation for reactants and transition states. The calculated values of ΔH are most probably underestimated, since only three active-site residues were included in the calculation. Nevertheless, a clear energetic superiority can be seen for the reaction catalyzed by the wild-type structure (in terms of activation energy) over the reactions catalyzed by either mutant structures. A similar result was obtained from experiment. A significant agreement between the experiment and the calculation was also obtained with the mutant Trp125→Arg (structure *tryptophans-m3*) when no activity with the mutant enzyme was observed by Kennes,[20] and at the same time the calculation of the reaction pathway failed due to the unfavorable orientation of reacting groups obtained in a very early step of the MOPAC/DRIVER calculation.

The structure *"tryptophans-m5"* represents the active site model of the haloalkane dehalogenase of the strain *Sphingomonas paucimobilis* UT26. One of the most significant differences observed for the substrate specificity of the *Xanthobacter* and *Sphingomonas* enzymes is that the latter enzyme cannot dehalogenate 1,2-dichloroethane. The increase in the activation energy barrier of about 7 kcal/mol calculated with the *tryptophans-m5* structure for 1,2-dichloroethane, compared with the barrier obtained with the wild-type (GJ10) structure, suggests that substitution in position 175 could be one of the structural features responsible for the differences in substrate specificity observed for GJ10 and UT26 dehalogenases.

The correlation between the experimentally determined values of V_{max} with the computed E^a values is qualitative only. This is not surprising, when the following limitations of the methodology we have used are taken into account: (i) calculations have been performed with only a few residues of the active site, (ii) the solvent has not been included in the calculations, (iii) the geometries close to the transition states have been identified, and (iv) mutant geometries *in nature* may be somewhat different from those we have obtained from minimization. The following approaches can be used for further improvements of the methodology: (i) the application of hybrid quantum-mechanical/molecular mechanical (QM/MM)[29,30] or empirical valence bond (EVB)[31] methods in which the complete enzyme surrounded by the solvent is included in the calculation and (ii) the use of an improved methodology for the preparation of mutant structures and refinements using, for example, fragment libraries and constrained molecular dynamics.

CONCLUSIONS

A number of semiemperical quantum chemical calculations for the first step of the S_N2 dehalogenation reaction have been performed. Animation of the reaction revealed the importance of two tryptophan residues (Trp125 and Trp175) for the reaction course. The significance of these two active site residues for the stabilization of the halide ion was previously proposed by Verschueren et al.,[16] based on a crystallographic and fluorescence study. An additional active-site residue, Phe172, has been identified as being important for the same kind of stabilization based on the changes in atomic charges during the reaction course. Monitoring of the changes in atomic charges during the reaction provides a very simple but effective method to elucidate the essential electrostatic interactions between enzyme and substrate and can assist in the identification of the catalytically important active-site residues.

The influence of the tryptophan residues on the kinetics and thermodynamics of the first dehalogenation reaction step has been further investigated by MOPAC/DRIVER calculations performed with starting geometries of different compositions and complexities. A decrease in the reaction activation energy of almost 10 kcal/mol was observed when both tryptophans and the nucleophile were included in the calculation when compared with the calculations containing the nucleophile only.

The MOPAC/DRIVER calculations have also been applied to the model structures of the haloalkane dehalogenase mutants which were experimentally prepared and studied by Kennes and co-workers.[20] Lower activation energy barriers were obtained for the reaction "catalyzed" by the wild-type enzyme residues when compared to its single point mutants. Our result is consistent with that obtained by Kennes, who observed very low dehalogenation activity of the same mutants in experiments with 1,2-dichloroethane and 1,2-dibromoethane. The agreement with experiment is qualitative only, since the experimentally observed differences in the catalytic activities among mutants could not be repro-

duced. The limitations of the computational and modeling method used in this study have been discussed, and necessary modifications leading toward more satisfactory results have been suggested. The most significant drawback of the methodology applied in this study is that the calculations were performed on a small model system *in vacuum* neglecting the effect of the surrounding protein and solvent. The calculated energies have therefore been used only for the relative comparison of the effect of single point mutations on activation barriers in the first reaction step.

An improved method similar to ours (in combination with some other molecular modeling methods) could possibly be used for the study of *in vivo* and *in vitro* mutational events ensuring the molecular evolution of degrading capabilities in bacteria. For this purpose, the proposed structure of another haloalkane dehalogenase, the enzyme of *Sphingomonas paucimobilis* UT26, has also been included in the calculations. The practical application of such a methodology for the design of genetically modified organisms with improved degrading abilities is possible.

ACKNOWLEDGMENT

We would like to acknowledge the authors of the XMol program from the Minnesota Supercomputer Center, Minneapolis for making their program freely available via the Internet. Computationally extensive calculations have been performed on the computing facilities of the Czech Academic Supercomputer Centre in Brno and Prague. Our thanks go to its operators. This work has been carried out under the framework of the project "Quantitative Structure−Activity Relationships for Predicting Fate and Effects of Chemicals in the Environment". This project is financially supported by the Environmental Technologies RTD Program (DG XII/D-1) of the Commission of the European Union under contract number EV5V-CT92-0211. Additional funding has been obtained via the EU Programme on Science and Technology Co-operation with Central and Eastern European countries under the supplementary agreement number CIPD-CT93-0042. Mary Lynam (Department of Civil and Environmental Engineering, The University of Michigan) is gratefully acknowledged for help with the linguistic revision of the manuscript.

REFERENCES AND NOTES

(1) Alexander, M. Biodegradation of Chemicals of Environmental Concern. *Science* **1981**, *211*, 132−138.
(2) Providenti, M. A.; Lee, H.; Trevors, J. T. Selected Factors Limiting the Microbial Degradation of Recalcitrant Compounds. *J. Industrial Microbiol.* **1993**, *12*, 379−395.
(3) Damborský, J. A Mechanistic Approach to Deriving Quantitative Structure−Activity Relationship Models for Microbial Degradation of Organic Compounds. *SAR QSAR Environ. Res.* **1996**, *5*, 27−36.
(4) Damborský, J.; Manová, K.; Kutý, M. In *Biodegradability Prediction*; Peijnenburg W. J. G. M., Damborský, J., Eds.; Kluwer Academic Publishers: Dordrecht, 1996; Chapter 8, p 75.
(5) Cohen, N. C.; Blaney, J. M.; Humblet, C.; Gund, P.; Barry, D. C. Molecular Modeling Software and Methods for Medicinal Chemistry. *J. Med. Chem.* **1990**, *33*, 883−894.
(6) Paulsen, M. D.; Ornstein, R. L. Active-Site Mobility Inhibits Reductive Dehalogenation of 1,1,1-Trichloroethane by Cytochrome P450cam. *J. Comput.-Aid. Mol. Design* **1994**, *8*, 389−404.
(7) Kubinyi, H. *3D QSAR in Drug Design*; ESCOM: Leiden, 1993.
(8) Mulholland, A. J.; Grant, G. H.; Richards, W. G. Computer Modeling of Enzyme Catalyzed Reaction Mechanisms. *Prot. Engineer.* **1993**, *6*, 133−147.
(9) Janssen, D. B.; Scheper, A.; Dijkhuizen, L.; Witholt, B. Degradation of Halogenated Aliphatic Compounds by *Xanthobacter autotrophicus* GJ10. *Appl. Environ. Microbiol.* **1985**, *49*, 673−677.
(10) Keuning, S.; Janssen, D. B.; Witholt, B. Purification and Characterization of Hydrolytic Haloalkane Dehalogenase from *Xanthobacter autotrophicus* GJ10. *J. Bacteriol.* **1985**, *163*, 635−639.
(11) Janssen, D. B.; Pries, F.; Van der Ploeg, J.; Kazemier, B.; Terpstra, P.; Witholt, B. Cloning of 1,2-Dichloroethane Degradation Genes of *Xanthobacter autotrophicus* GJ10 and Expresion and Sequencing of the dhlA Gene. *J. Bacteriol.* **1989**, *171*, 6791−6799.
(12) Tardif, G.; Greer, C. W.; Labbe, D.; Lau, P. C. K. Involvement of a Large Plasmid in the Degradation of 1,2-Dichloroethane by *Xanthobacter autotrophicus*. *Appl. Environ. Microbiol.* **1991**, *57*, 1853−1857.
(13) Franken, S. M.; Rozeboom, H. J.; Kalk, K. H.; Dijkstra, B. W. Crystal Structure of Haloalkane Dehalogenase: an Enzyme to Detoxify Halogenated Alkanes. *EMBO J.* **1991**, *10*, 1297−1302.
(14) Verschueren, K. H. G.; Franken, S. M.; Rozeboom, H. J.; Kalk, K. H.; Dijkstra, B. W. Refined X-ray Structures of Haloalkane Dehalogenase at pH 6.2 and pH 8.2 and implications for the Reaction Mechanism. *J. Mol. Biol.* **1993**, *232*, 856−872.
(15) Verschueren, K. H. G.; Seljee, F.; Rozeboom, H. J.; Kalk, K. H.; Dijkstra, B. W. Crystallographic Analysis of the Catalytic Mechanism of Haloalkane Dehalogenase. *Nature* **1993**, *363*, 693−698.
(16) Verschueren, K. H. G.; Kingma, J.; Rozeboom, H. J.; Kalk, K. H.; Janssen, D. B.; Dijkstra, B. W. Crystallographic and Fluorescence Studies of the Interaction of Haloalkane Dehalogenase with Halide Ions. Studies with Halide Compounds Reveal a Halide Binding Site in the Active Site. *Biochemistry* **1993**, *32*, 9031−9037.
(17) Pries, F.; Kingma, J.; Pentega, M.; Van Pouderoyen, G.; Jeronimus-Stratingh, C. M.; Bruins, A. P.; Janssen, D. B. Site-directed Mutagenesis and Oxygen Isotope Incorporation Studies of the Nucleophilic Aspartate of Haloalkane Dehalogenase. *Biochemistry* **1994**, *33*, 1242−1247.
(18) Pries, F.; Kingma, J.; Janssen, D. B. Activation of an Asp-124→Asn Mutant of Haloalkane Dehalogenase by Hydrolytic Deamidation of Asparagine, *FEBS Lett.* **1995**, *358*, 171−174.
(19) Pries, F.; Kingma, J.; Krooshof, G. H.; Jeronimus-Stratingh, C. M.; Bruins, A. P.; Janssen, D. B. Histidine 289 is Essential for Hydrolysis of the Alkyl-enzyme Intermediate of Haloalkane Dehalogenase. *J. Biol. Chem.* **1995**, *270*, 10405−10411.
(20) Kennes, C.; Pries, F.; Krooshof, G. H.; Bokma, E.; Kingma, J.; Janssen, D. B. Replacement of Tryptophan Residues in Haloalkane Dehalogenase Reduces Halide Binding and Catalytic Activity. *Eur. J. Biochem.* **1995**, *228*, 403−407.
(21) Stewart, J. J. P. *MOPAC Manual v 6.0*; Quantum Chemistry Program Exchange: Indiana, 1990.
(22) Černohorský, M.; Kutý, M.; Koča, J. A Multidimensional Driver for Quantum Chemistry Program MOPAC. *Computers Chem.* **1997**, *21*, 35−44.
(23) Nagata, Y.; Nariya, T.; Ohtomo, R.; Fukuda, M.; Yano, K.; Takagi, M. Cloning and Sequencing of a Dehalogenase Gene Encoding an Enzyme with Hydrolase Activity Involved in the Degradation of Hexachlorocyclohexane in *Pseudomonas paucimobilis*. *J. Bacteriol.* **1993**, *175*, 6403−6410.
(24) Damborský, J.; Bull, A. T.; Hardman, D. J. Homology Modeling of the Haloalkane Dehalogenase of *Sphingomonas paucimobilis* UT26. *Biologia* **1995**, *50*, 523−528.
(25) Ford, G. P.; Wang, B. Incorporation of Hydration Effects within Semiempirical Molecular Orbital Framework. AM1 and MNDO Results for Neutral Molecules, Cations, Anions and Reacting Systems. *J. Am. Chem. Soc.* **1992**, *114*, 10563−10569.
(26) Dewar, M. J. S.; Storch, D. M. Alternative View of Enzyme Reactions. *Proc. Natl. Acad. Sci. U.S.A.* **1985**, *82*, 2225−2229.
(27) Alex, A.; Clark, T. MO-Studies of Enzyme Reaction Mechanisms. I. Model Molecular Orbital Study of the Cleavage of Peptides by Carboxypeptidase A. *J. Comput. Chem.* **1992**, *13*, 704−717.
(28) Fersht, A. R.; Serrano, L. Principles of Protein Stability Derived from Protein Engineering Experiments. *Curr. Opin. Struct. Biol.* **1993**, *3*, 75−83.
(29) Bash, P. A.; Field, M. J.; Karplus, M. Free Energy Perturbation Method for Chemical Reactions in the Condensed Phase: A Dynamical Approach Based on a Combined Quantum and Molecular Mechanics Potential. *J. Am. Chem. Soc.* **1987**, *109*, 8092−8094.
(30) Bash, P. A.; Field, M. J.; Davenport, R. C.; Petsko, G. A.; Ringe, D.; Karplus, M. Computer Simulation and Analysis of the Reaction Pathway of Triosephosphate Isomerase. *Biochemistry* **1991**, *30*, 5826−5832.
(31) Aqvist, J.; Fothergill, M; Warshel, A. Computer Simulation of the CO_2/HCO^{3-} Interconversion Step in Human Carbonic Anhydrase I. *J. Am. Chem. Soc.* **1993**, 115, 631−635.

CI960483J